Preliminary Studies on Vascular Network Quantification in Chick Chorioallantoic Membrane Images

Leandro T. De La Cruz, Nina S. T. Hirata
Institute of Mathematics and Statistics
University of São Paulo
São Paulo - Brasil
www.ime.usp.br/∼{lticlia,nina}

***Abstract*—Angiogenesis is a natural process of new vessel formation from existing ones. Due to its role in diseases such as in tumor growth, angiogenesis assays are performed to understand the effects of angiogenic and anti-angiogenic agents. A widely used *in vivo* model, due to its rich vascular network, is the chick chorioallantoic membrane (CAM). In order to quantify angiogenesis, objective measures that allow comparison of observed vascular networks are needed. In this work we investigate vascular network quantification in CAM microscopic images. Some common quantification metrics as well as metrics from other domains for the quantification of angiogenesis in CAM images are described and then computed on a small set of sample images.**

***Keywords*-Chick Chorioallantoic Membrane; Angiogenesis quantification; Vascular network; Feature extraction.**

I. Introduction

Angiogenesis is a natural process of new vessel formation from existing ones. The phenomenon is observed in normal biological development and in wound healing processes, but it is also related to diseases such as cancer, rheumatoid arthritis, diabetic retinopathy, among others [1]. Several angiogenesis assays to study the effects of angiogenic and anti-angiogenic agents are used [2]. Among them, a widely used *in vivo* model is the chick chorioallantoic membrane (CAM). This model is recommended due to its rich vascular network and because it allows *in vivo* interaction during the embryo growth. Besides, CAM appears to be easier to handle and less expensive than other *in vivo* models [3].

Quantification of angiogenesis is at large extent still done manually. Besides being a tiring task, manual quantification may be highly subjective and thus affect comparative studies. In order to obtain objective quantification measures, approaches based on automated processing of optical microscopy images of chick CAM images are being proposed [4], [5]. Fig. 7 shows an egg and a microscope slide with CAM.

Image processing approaches for quantification of angiogenesis in CAM images are typically comprised of three steps: vascular network segmentation, extraction of measures from the detected features and validation of the obtained measures. The whole process is schematized in Fig. 2.

Simple measures such as vessel area density and density of vessel extremities are usually computed [4], [5]. In addition,

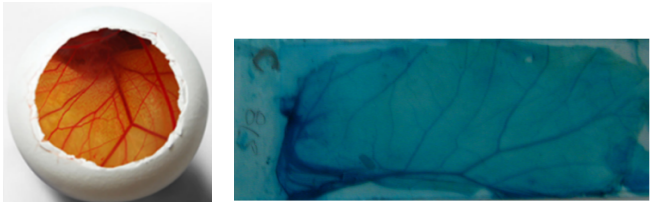

(a) Egg (b) Membrane on a slide

Fig. 1. Chick chorioallantoic membrane

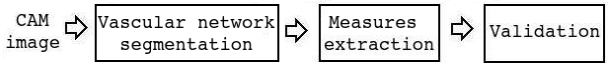

Fig. 2. General scheme for angiogenesis quantification in CAM images

other measures such as fractal dimension [6] are also used. To quantify microvasculature regions, texture information (e. g. contrast, correlation and entropy) are used [4], [5]. However many of these measures are highly affected by the quality of the image (resolution).

In this work we report an ongoing work on vascular network quantification in CAM images. We list some of the metrics frequently cited in the related literature and also in studies of different application domains such as hydrology (river), botany (plant leaves), and pulmonary bronchial system. Some preliminary results for different quantification metrics applied to CAM images are presented and discussed. The final goal of this work is to establish a robust set of metrics to quantify angiogenesis in CAM images.

II. Vascular network feature detection

In order to quantify vascular network, first some structural features should be identified in the network image. Given a CAM image, let us denote by f the corresponding binary image containing the skeleton of the segmented vascular network. Fig. 3 shows a CAM image and the skeleton of the vascular network. Network features described hereafter are all extracted from the skeleton image.

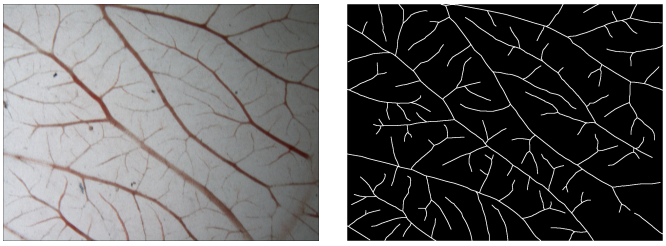

(a) CAM image-6 (b) Skeleton

Fig. 3. CAM image and skeleton of its vascular network

A. End points

An end point is a pixel p in the skeleton that has just one neighbor that is also in the skeleton. Formally, end points can be expressed by the following function:

$$[\rho(f)](p) = \begin{cases} 1, & \text{if } f(p) = 1 \text{ and } \sum_{q \in N_8(p)} f(q) = 1 \\ 0, & \text{otherwise,} \end{cases} \tag{1}$$

where $N_8(p)$ denotes the set of 8-connected neighbors of p.

B. Branching point

A pixel $p \in f$ is a branching point if it belongs to the skeleton, has exactly three neighbors (according to 8-connectivity) that are also in the skeleton, and its neighbors in the skeleton are not 4-connected. Thus, branching points can be defined by the following function:

$$[\xi(f)](p) = \begin{cases} 1, & \text{if } f(p) = 1 \text{ and } \sum_{q \in N_8(p)} f(q) = 3 \\ & \text{and } \forall p_1, p_2 \in N_8(p), p_1 \neq p_2, \\ & \text{if } f(p_1) = f(p_2) = 1 \rightarrow p_1 \notin N_4(p_2) \\ 0, & \text{otherwise,} \end{cases} \tag{2}$$

where $N_4(p)$ denotes the set of 4-connected neighbors of p.

Fig. 4 shows examples of end points and branching points.

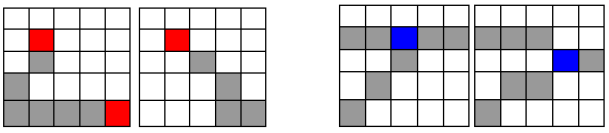

(a) End points (red color) (b) Branching points (blue color)

Fig. 4. Interesting points of vascular network skeleton

C. Classification of vessel segments

In hydrology, branching structures of rivers can be classified according to different taxonomies (e.g., Horton, Shreve, Strahler, Tokunaga and Hack taxonomies). Recent studies show that the Strahler [7] and Tokunaga [8], [9] taxonomies can be useful to characterize biological branching structures such as trees, leaves, and bronchial and cardiovascular systems [10].

Each segment connecting end points to branching points or branching points to branching points are analyzed from the lowest to the highest hierarchical levels, and class labels are assigned to each segment following some simple rules.

Strahler taxonomy: In the Strahler taxonomy (also known as "Horton-Strahler" taxonomy), each segment connected to an end point (except the root point) is classified as being of order 1. Then, other segments are labeled taking into consideration the labels of the two segments that converge at their starting point. If two segments of order k converge, the new segment is labeled as being of order $k+1$; if two segments with different order converge, then the order of the new segment is the higher one of the two converging segments. An example of this classification system is shown in Fig. 5.

Tokunaga taxonomy: In the Tokunaga taxonomy, each segment in the structure has two order values: a child value (v_c) and a father value (v_f). The v_c value corresponds to the Strahler order and the v_f value is the Strahler order of the other segment when convergence occurs [8]. An example of this classification system is shown in Fig. 5. This taxonomy is richer in the sense that it differentiates "bifurcation" from side branches, while Strahler taxonomy does not. It is applied on drainage network, but few applications in biology are reported.

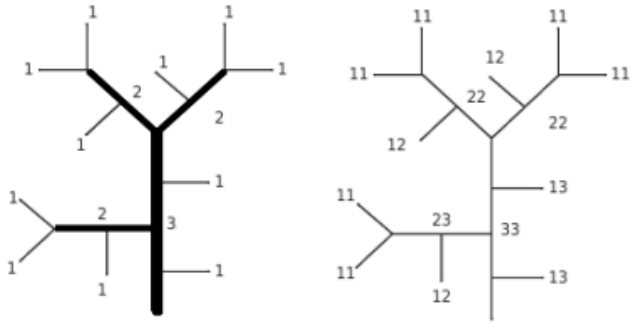

(a) Strahler taxonomy (b) Tokunaga taxonomy

Fig. 5. Classification systems (figures extracted from [9])

III. Quantification measure computation

A. Skeleton representation as a graph

In order to facilitate computation, we represent the vascular network skeleton as an undirected graph $G = (V, E)$, where $V = V_{end} \cup V_{bch}$ is a set of vertices composed by both ending (V_{end}) and branching (V_{bch}) points, and E is the set of edges corresponding to vessel skeleton segments between two points in V. After detecting end and branching points, the vertex set is created and then an adapted "depth-first search" algorithm is used to create the edges. The weight of each edge $e \in E$ is the number of pixels of the skeleton segment that corresponds to it.

Graph representation allows independent treatment of each component of the vascular network. It should be noted that since CAM images correspond to small regions of the whole membrane, often only fragments of the whole network are present in an image and thus that fact should be taken into consideration when measures are computed. Fig. 6 shows two

examples of graph representation of vascular networks. Red dots correspond to end points, while dark blue ones correspond to branching points. The color of the edges indicate graph components. Note also that most of the vertices close to the image boundary are not actual end points, but are included only to represent the skeleton segments as they are seen in the image.

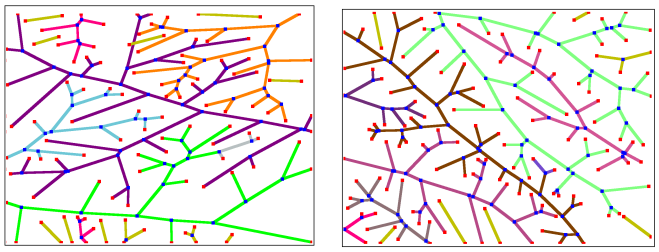

(a) Graphs generated from Fig. 7 (b) (b) Graphs generated from Fig. 7 (f)

Fig. 6. Representation of a vascular network skeleton as a graph.

B. Quantification measures

Let $m \times n$ be the dimensions in pixels of the skeleton image f. Some commonly used metric refers to the density of the network, of its skeleton, of end points and so forth.

- **Skeleton density:** $D_Z = \dfrac{\sum_{p \in f} f(p)}{m \times n}$. Closely related to this is the vessel density that considers not only skeleton but also the caliber of the vessels. However, vessel density depends much more than skeleton density on precise segmentation of the vessels.
- **Ending points density:** $D_{end} = \dfrac{|V_{end}|}{\sum_{p \in f} f(p)}$
- **Branching points density:** $D_{bch} = \dfrac{|V_{bch}|}{\sum_{p \in f} f(p)}$
- **Average length of segments of level i:** $L_i = \dfrac{\sum_{e \in E_i} weight(e)}{|E_i|}$, where E_i denotes the set of edges corresponding to segments of order i.

All metrics that involve number of pixels should be scaled according to image spatial resolution. This is not done in this work because all images considered have a same resolution.

Let $S_i = |E_i|$ be the total of segments of order i and let L_i be their mean length. Horton [11] introduced the branching ratio (R_S) and the length-order ratio (R_L) concepts, which are defined as follows:

$$R_S = \frac{S_i}{S_{i+1}} \quad , \quad R_L = \frac{L_{i+1}}{L_i} \tag{3}$$

Two of Horton's laws establish that both R_S and R_L are nearly constant for a range of stream order for all river network. These laws also apply to the Strahler taxonomy.

If we consider classification based on Tokunaga taxonomy, a branching-number matrix T can be built, where each element T_{ij} of T represents the total of segments with $v_c = i$ and $v_f = j$. Information in this matrix is useful to analyze the vascular network growth. For example, for the network in Fig. 5(b) we have that $T_{11} = 6$, $T_{12} = 3$ and $T_{13} = 2$, meaning that among eleven segments of order 1, three converge to segments of order 2, while two converge to segments of order 3.

Another useful measure is the spatial spreadness of the points of interest. To capture this information, let K be a positive integer and ε be a positive number in $\mathbb{R}$. Then, we define for any end point p:

$$K_\varepsilon(p) = |\{q \in V_{end} : \|q - p\| \leq \varepsilon\}|$$

and

$$\varepsilon_K(p) = min\{\varepsilon \in \mathbb{R} : K_\varepsilon(p) \geq K\}$$

These values can be averaged considering all end points in the image. Thus, given f, we define $\overline{K_\varepsilon}(f) = \frac{1}{|V_{end}|} \sum_{p \in V_{end}} K_\varepsilon(p)$ and $\overline{\varepsilon_K}(f) = \frac{1}{|V_{end}|} \sum_{p \in V_{end}} \varepsilon_K(p)$.

IV. Preliminary Results and Discussion

The measures presented above were computed for manually segmented vascular networks of 7 CAM images shown in Fig. 7. The obtained values are shown in Table I. These measures, as they are single values, correspond to poor representations of network structure. Instead, more representative

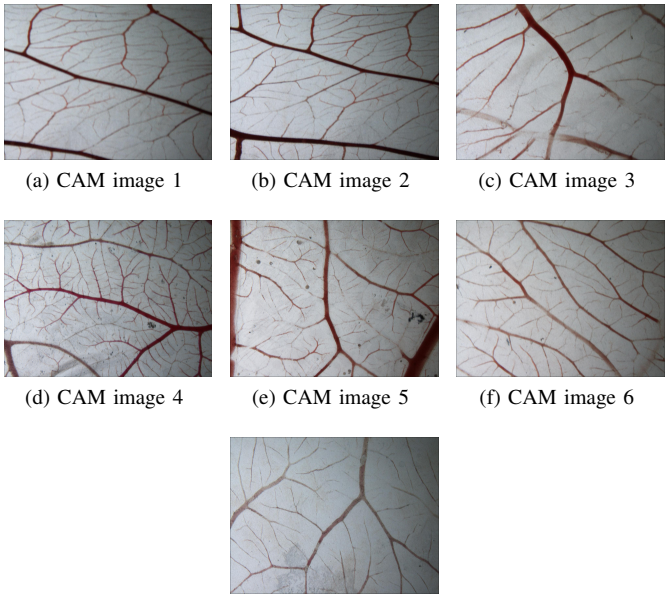

(a) CAM image 1 (b) CAM image 2 (c) CAM image 3

(d) CAM image 4 (e) CAM image 5 (f) CAM image 6

(g) CAM image 7

Fig. 7. Set of 7 CAM images

TABLE I
Quantification metrics: expressed in percentage

CAM img.	D_Z	D_{end}	D_{bch}
1	1.133	0.667	0.557
2	1.391	0.649	0.450
3	0.662	0.578	0.258
4	0.918	0.540	0.420
5	1.027	0.745	0.578
6	1.301	0.795	0.619
7	0.884	0.616	0.322

information can be obtained using measures such as the R_S and R_L ratios.

Branching and length-order ratio for segments classified according to the Strahler taxonomy are shown in Fig. 8 and Fig. 9, respectively. As can be seen in the figures, CAM

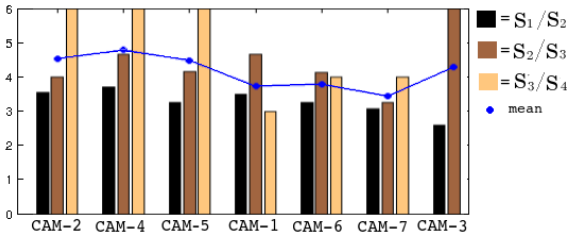

Fig. 8. Branching ratios of 7 CAM images

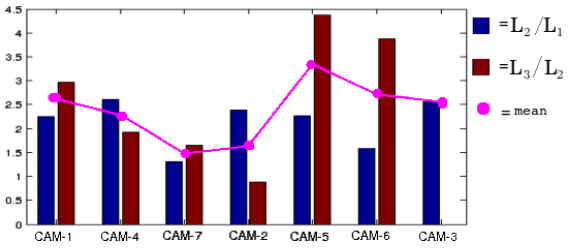

Fig. 9. Length-order ratios of 7 CAM images

images 1 and 7 satisfy fairly well the two Horton's laws, while others satisfy only one or none of them. However, these measures should be looked cautiously since each CAM image corresponds to only a small region of the whole membrane.

The spreadness of end points are represented by $\varepsilon \times \overline{K}_\varepsilon$ and $K \times \overline{\varepsilon}_K$ graphs shown in Fig. 10 and Fig. 11, respectively. Note that CAM images 1, 2, 5 and 6 present very similar spreadness curve in accordance with what can be observed in the images.

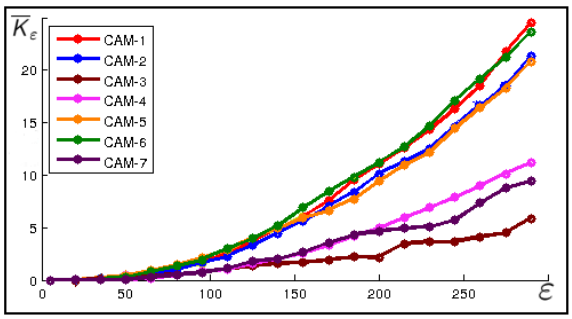

Fig. 10. Spreadness of the ending points

V. Future works

Results obtained so far indicate that even in membranes of chick embryo from similar biological and environmental conditions, the single valued measures vary significantly from image to image. On the other hand, metrics such as segment

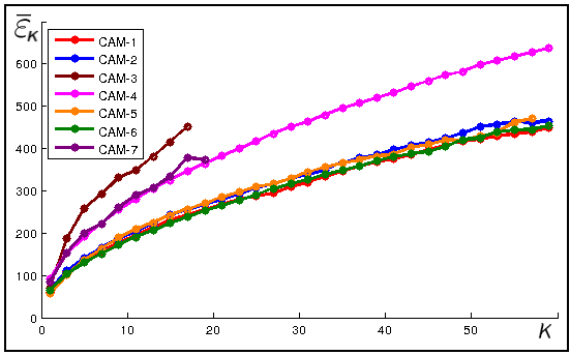

Fig. 11. Spread of the ending points

ratios and spreadness graphs seem to be able to capture structural and spatial information of the vascular network.

An important issue to be tackled is the validation of the measures. Some of the future steps include investigation of additional metrics and comparison of the measures between normal chick embryos (control) and treated embryos, aiming to find a set of metrics that can be useful to quantity angiogenesis robustly.

Acknowledgment

We would like to thank CNPq and CAPES for supporting this work, and Dr. Ligia F. Gomes for providing us the CAM images.

References

[1] N. Ferrara and R. S. Kerbel, "Angiogenesis as a therapeutic target," *International Weekly Journal of Science*, vol. 438, pp. 967–974, 2005.

[2] R. Auerbach, R. Lewis, B. Shinners, L. Kubai, and N. Akhtar, "Angiogenesis assays: A critical overview," *Clinical Chemistry*, vol. 49, no. 1, pp. 32–40, 2003.

[3] D. Ribatti, A. Vacca, L. Roncali, and F. Dammacco, "The chick embryo chorioallantoic membrane as a model for in vivo research on angiogenesis," *The International Journal of Developmental Biology*, vol. 40, pp. 1189–1197, 1996.

[4] S. Blacher, L. Devy, R. Hlushchuck, E. Larger, N. Lamandé, P. Burri, P. Corvol, V. Djonov, J. M. Foidart, and A. Noel, "Quantification of angiogenesis in the chicken chorioallantoic membrane (CAM)," *Image Analysis & Stereology*, vol. 15, pp. 169–180, 2005.

[5] C. N. Doukas, I. Maglogiannis, and A. A. Chatziioannou, "Computer-supported angiogenesis quantification using image analysis and statistical averaging," *IEEE Transactions on Information Technology in Biomedicine*, vol. 12, no. 5, pp. 650–657, 2008.

[6] C. Dimitropoulou, M. Maragoudakis, and M. Konerding, "Effects of thrombin and of the phospholipase c inhibitor, d609, on the vascularity of the chick chorioallantoic membrane," *General Pharmacology*, vol. 35, pp. 241–147, 2002.

[7] A. N. Strahler, "Dynamic basis of geomorphology," *Geological Society of America Bulletin*, vol. 63, no. 9, pp. 923–938, 1952.

[8] E. Tokunaga, "Ordering of divide segments and law of divide segment numbers," *Transactions, Japanese Geomorphological Union*, vol. 5, pp. 71–76, 1984.

[9] D. L. Turcotte, J. D. Pelletier, and W. I. Newman, "Networks with side branching in biology," *Journal of Theoretical Biology*, vol. 193, no. 4, pp. 577–592, 1988.

[10] G. Kassab, "Scaling laws of vascular trees: of form and function," *American Journal of Physiology-heart and Circulatory Physiology*, vol. 290, no. 2, pp. 894–903, 2005.

[11] R. E. Horton, "Erosional development of streams and their drainage basins; hydrophysical approach to quantitative morphological," *Geological Society of America Bulletin*, vol. 56, no. 3, pp. 275–370, 1945.